2025-32-0016/20259216 Published 03 Nov 2025

Overcoming Challenges in Motorcycle Exhaust Flow Measurement: A Study on Measurement Accuracy and Systematic Effects of an Annubar-Based Approach

Sebastian Schurl Graz University of Technology

Christian Hafenmayer and Mathias Lankau AIP GmbH & Co. KG

Günter Brenn, Stephan Schmidt, and Roland Kirchberger Graz University of Technology

Citation: Schurl, S., Hafenmayer, C., Lankau, M., Brenn, G. et al., "Overcoming Challenges in Motorcycle Exhaust Flow Measurement: A Study on Measurement Accuracy and Systematic Effects of an Annubar-Based Approach," SAE Technical Paper 2025-32-0016, 2025, doi:10.4271/2025-32-0016.

Received: 04 Jun 2025 Revised: 01 Jul 2025 Accepted: 07 Jul 2025

Abstract

Accurate exhaust mass flow measurement is critical for Real Driving Emission (RDE) testing; however, it is particularly challenging for motorcycles due to variations in chemical composition, strong pulsations and even reverse flow effects at low engine speeds. Traditional differential pressure-based flow meters often struggle under these conditions, particularly in low-speed and low-load operation. This study evaluates the feasibility and accuracy of an Annubar-based exhaust flow meter (EFM) designed to address these challenges by means of assessing eight motorcycles with single-, two-, and four-cylinder engine configurations. The EFM performance is evaluated via correlation analysis with laboratory-grade reference instruments and engine control unit (ECU) data. Additionally, systematic effects such as pulsation behavior, spectrogram analysis, and the influence of engine load and speed are investigated.

The results demonstrate a strong correlation between EFM and reference measurements, indicating the EFM potential as a viable exhaust mass flow measurement solution. However, systematic deviations were observed, particularly at low engine speeds and loads, where pulsation effects caused oscillatory measurement behavior. These deviations stem from the interaction between engine-induced pulsations and the EFM response characteristics. To mitigate these effects, advanced filtering techniques and engine-aware compensation strategies, leveraging engine RPM and load data, are proposed to enhance measurement stability and accuracy. These improvements could make EFMs a more reliable tool for motorcycle RDE assessments, enhancing real-world emission testing methodologies.

Introduction

Accurately measuring exhaust mass flow in motorcycle engines remains a significant challenge, particularly in the context of RDE testing [1, 2, 3]. Unlike automotive engines, motorcycle engines are typically characterized by a small number of cylinders, longer ignition intervals, and an unfavorable ratio of engine displacement to exhaust system volume. These factors lead to pronounced pulsations in exhaust mass flow, further complicated by high concentrations of condensable water vapor, particulate matter, and variable chemical compositions.

Conventional exhaust flow measurement techniques, such as differential pressure-based methods, struggle to maintain accuracy under these dynamic conditions. This is especially critical at low engine speeds, where flow reversals can occur, introducing additional measurement uncertainties. The limitations of existing measurement approaches highlight the need for a more reliable and precise method to ensure the accuracy of RDE testing for motorcycles—an essential aspect of regulatory compliance and environmental impact assessment.

This study evaluates the potential of an Annubar-based EFM as a solution to these challenges. By assessing its performance under the specific operating conditions of various motorcycle engines, this research aims to provide insights into the feasibility of Annubar technology for improving exhaust flow measurement accuracy in RDE applications. Accurately measuring exhaust mass flow in

motorcycle engines remains a significant challenge, particularly in the context of RDE testing [1, 2, 3]. Unlike automotive engines, motorcycle engines are typically characterized by a small number of cylinders, longer ignition intervals, and an unfavorable ratio of engine displacement to exhaust system volume. These factors lead to pronounced pulsations in exhaust mass flow, further complicated by high concentrations of condensable water vapor, particulate matter, and variable chemical compositions.

Conventional exhaust flow measurement techniques, such as differential pressure-based methods, struggle to maintain accuracy under these dynamic conditions. This is especially critical at low engine speeds, where flow reversals can occur, introducing additional measurement uncertainties. The limitations of existing measurement approaches highlight the need for a more reliable and precise method to ensure the accuracy of RDE testing for motorcycles—an essential aspect of regulatory compliance and environmental impact assessment.

This study evaluates the potential of an Annubar-based EFM as a solution to these challenges. By assessing its performance under the specific operating conditions of various motorcycle engines, this research aims to provide insights into the feasibility of Annubar technology for improving exhaust flow measurement accuracy in RDE applications. In addition to its measurement characteristics, the Annubar approach is also attractive for mobile testing due to its compact design, relatively low cost, and minimal impact on engine backpressure, making it particularly suitable for applications in the motorcycle segment.

Challenges in Exhaust Flow Measurement for Motorcycles

The assessment of exhaust mass flow in motorcycle engines is complicated by the unique flow dynamics inherent to combustion engines. Unlike steady-state flow systems, exhaust flow in internal combustion engines is highly unsteady, exhibiting strong pulsations due to the periodic nature of the combustion cycle. These pulsations consist of high-amplitude pressure waves, primarily triggered by the opening of the exhaust valve (EVO), followed by secondary compression and expansion waves traveling through the exhaust system [2,4, 5, 6], as shown in Figure 1. The propagation of these waves is further influenced by exhaust system geometry, including manifolds, catalytic converters, and mufflers, leading to complex interactions such as wave reflection, refraction, and attenuation [7].

Conventional exhaust flow measurement techniques, such as differential pressure-based Pitot tubes, face inherent limitations in capturing these pulsating flow characteristics. The fundamental issue arises from the square-root dependency of flow velocity on pressure differential (1), which causes errors when averaging pressure as well as density fluctuations in unsteady flow conditions [9,10].

$$v = k_p \sqrt{\frac{2\left(p_T - p_S\right)}{\rho}} \tag{1}$$

FIGURE 1 crank angle resolved pressure pulse indicating the two pulses of EVO and piston motion [8]

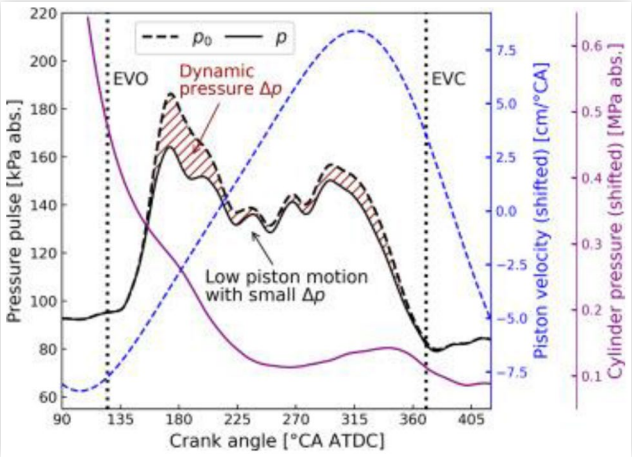

Moreover, the exhaust flow profile within the pipe varies significantly: while turbulent flow exhibits a relatively uniform velocity distribution, laminar flow is highly non-uniform, with peak velocities at the center and near-zero velocities at the pipe walls [4]. These variations further complicate single-point measurement accuracy, making conventional Pitot tubes unreliable in highly dynamic exhaust conditions. To improve measurement accuracy, averaging Pitot tube configurations such as the Annubar have been introduced. By incorporating multiple sensing points across the flow cross-section, Annubar-based EFM reduce sensitivity to local turbulence and pulsation effects. The Environmental Protection Agency (EPA) has endorsed such devices for onboard exhaust flow measurement in passenger cars and heavy-duty applications, demonstrating their reliability under real-world conditions [4]. However, the effectiveness of Annubar technology in motorcycle exhaust systems—characterized by extreme pulsation intensities and complex pressure wave interactions—remains largely unverified.

This study systematically evaluates the performance of an Annubar-based EFM tailored for motorcycle applications, addressing its suitability for highly unsteady exhaust flow conditions.

Methodology

Equipment – 1.5” LF EFM

The EFM used in this study is an 1.5" Low-Flow (LF) EFM, specifically designed for applications with low exhaust mass flow rates, such as motorcycle engines. As illustrated in Figure 2, the EFM consists of a long metal tube with 90° bends on both sides, housing the necessary electronics and sensors. It is designed for easy integration into exhaust systems using v-band clamps and can be connected via stiff or flexible metal tubing. Heated hoses can be directly attached to the internal probes via

FIGURE 2 AIP 1.5" LF-EFM

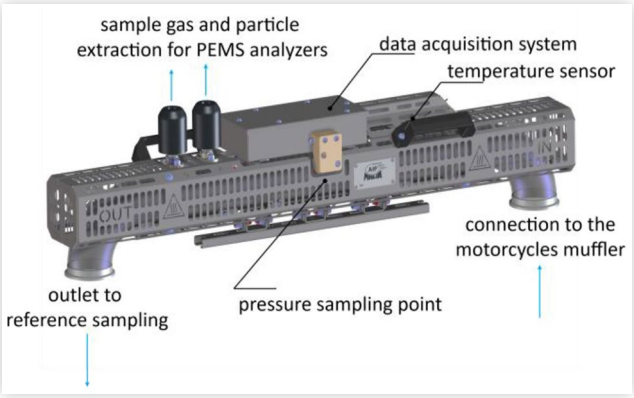

a quick-lock system, allowing for tool-free installation and rapid integration with Portable Emissions Measurement Systems (PEMS).

The EFM operates according to the Annubar working principle, utilizing differential pressure measurement across an averaging Pitot tube. To enhance measurement precision over a wide range of exhaust flow rates, the system employs an array of pressure sensors in a cascade configuration. Additionally, exhaust gas density is continuously calculated by monitoring absolute pressure and temperature within the tube, ensuring accurate mass flow determination.

Sampling and processing occur internally at rates of up to 5 kHz, allowing for high-frequency data acquisition in pulsative flow regimes. Integrated digital filtering techniques effectively smooth the signal, mitigating the effects of pulsations, which are particularly pronounced in low-cylinder-count engines. The EFM is available in different sizes, ranging from 1.5" to 4", with the choice of size dependent on the expected exhaust mass flow of the engine.

For this study, the 1.5" LF-EFM variant was selected due to its specialized probe, optimized for low-flow applications. This configuration ensures reliable measurement performance in motorcycle exhaust systems, where conventional EFMs may struggle due to the highly dynamic nature of the flow. Table 1 summarizes the key specifications of the AIP 1.5" LF-EFM.

TABLE 1 specifications of the 1.5" LF-EFM

Exhaust Gas Temperature	0 °C – 700 °C
Accuracy	2 % of reading or 0.3 % of full scale; whichever is larger
Precision (Repeatability)	≤ 1 % of full scale
Noise	≤ 2 % of full scale
Zero Drift/ Span Drift	≤ 2 % of full scale over 4 h
Measuring Range	0.6 g/s – 57 g/s
Mass	< 6 kg
L x W x H	600 x 150x 300 mm

Test Setup

The setup for the exhaust flow measurement was designed to benchmark the 1.5" LF EFM against a reference system using Constant Volume Sampler (CVS) and ECU data as shown in Figure 3. The experimental arrangement features a motorcycle mounted securely on a chassis dynamometer, where it was driven through a predefined test cycle [11] simulating typical operating conditions. The exhaust gases were directed through a metal hose connected to the EFM, which measured the exhaust flow rate.

The exhaust outlet flow from the EFM was sampled by the CVS system within the dynamometer's dilution tunnel, according the type-approval process for emission testing. To minimize the influence of the exhaust gas sampling on the flow dynamics and ensure accurate mass flow measurement, an open CVS system was used during the tests.

The CVS system operates by drawing a constant volumetric flow through a dilution tunnel, where the exhaust gases are mixed with ambient air. This method enables precise measurement of pollutant concentrations and exhaust volume flow under dynamic engine operation, and serves as the regulatory reference method for emissions certification [12].

Furthermore, a Controller Area Network (CAN) interface connected to the vehicle ECU allowed for real-time monitoring of critical engine parameters such as engine speed and load, providing valuable insights into the dynamic behavior of the engine and its impact on the exhaust flow measurement, described later in this section.

The exhaust mass flow rate was calculated following EU Regulation No 134/2014 [14]. The primary equation for determining the dilution factor (DF) is as follows:

$$DF = \frac{X}{C_{CO_2} + C_{CO} + C_{HC}} \quad (2)$$

where:

- X...represents the CO_2 concentration in the exhaust at stoichiometric conditions.
- C_i...diluted concentration in vol%

FIGURE 3 chassis dyno setup for the benchmark investigations [13]

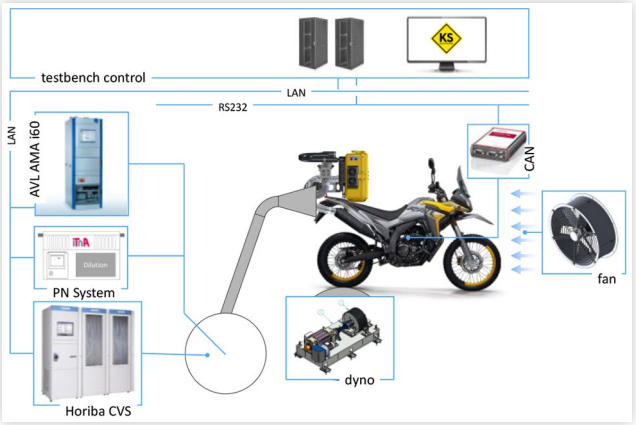

This equation approximates the dilution factor assuming stoichiometric combustion and thus a carbon dioxide concentration of e.g., X = 13.4% for gasoline E5. To gain additional accuracy, raw emission measurement of carbonaceous species can be applied to substitute the estimated X by the sum of raw exhaust concentrations of CO_2, CO and THC.

The assessment of the dilution factor based on the DF formula serves as a good approximation of the real dilution ratio (DR) which is based on the flow rates themselves:

$$DR = \frac{\dot{V}_{CVS}}{\dot{V}_{exh}} \tag{3}$$

The assessment of $\dot{V}_{exh}$ using the outlined equation (3) serves as a reference for the following verification of the EFM measured flow. To ensure the accuracy of the reference, several key factors affecting the measurement accuracy were recognized and carefully monitored, including:

- Analyzer Response Time: Emission analyzers, with inherent response times, can introduce delays in correlating emissions concentrations with actual flow rates. These delays have been assessed and compensated.
- Inverse PT1 Correction: Emission analyzers act as low-pass filters, smoothing higher-frequency signals. Inverse PT1 correction was applied to restore sharp transients and improve the accuracy of the measurements.
- Leakages: Potential leaks in the CVS system, especially at connections or seals, were accounted for by conducting Critical Flow Orifice (CFO) checks to eliminate inaccuracies.
- Analyzer Calibration: All analyzers were rigorously calibrated to minimize errors in the measurement process.

In addition to the emission-based reference, open-access data from the ECU - retrieved via the standardized On-Board Diagnostics (OBD) interface - can be utilized to support and extend these investigations. This is particularly valuable for motorcycles that do not feature a Mass Air Flow (MAF) sensor.

In such cases, the Speed-Density method is applied to estimate the intake air mass flow using available sensor data such as manifold absolute pressure (MAP), intake air temperature (MAT), and engine speed, combined with a model of the engine's volumetric efficiency.

A key OBD parameter defined in SAE J1979 is the Calculated Load Value (CEL, PID 04), which provides a normalized indication of engine load, is direct proportional to the current air flow and therewith well suited as additional reference, as speed density faces difficulties for motorcycle engines [15]. It is defined as:

$$CEL = \frac{current\ airflow}{peak\ airflow\left(WOT\ at\ STP\right) \cdot \frac{p}{p_0} \cdot \sqrt{\frac{T_0}{T}}} \tag{4}$$

By leveraging standard OBD parameters such as the Calculated Load Value it is possible to estimate intake, further exhaust mass flow rates without direct air mass measurements. This enables an effective non-invasive and therewith widely applicable or even standardized method for analysis using readily accessible ECU data, with respect to some simplifications outlined in Schurl et al. [15].

Test vehicles

The following Table 2 presents a selection of motorcycles that differ primarily in terms of engine architecture. This selection was made to ensure that it is representative of the overall fleet of motorcycles within the L3e category. Mopeds in the L1e category and enduro vehicles were excluded due to the current difficulties in using full functional PEMS equipment on these vehicles is already proving very difficult and alternative methods are being developed [15].

All of the motorcycles listed are equipped with modern 4-stroke, 4-valve engines featuring controlled exhaust aftertreatment and Port Fuel Injection (PFI) technology. Each vehicle complies with the EU5 emission standard and is equipped with an OBD system for comprehensive emissions control, allowing access to some engine data.

The selection includes motorcycles with different engine configurations, ranging from single-cylinder engines to multi-cylinder engines. These vehicles also feature varying displacement and ignition timing characteristics. The ignition spacing (in degrees crank angle, °CA) highlights the differences in firing intervals, which are characteristic of single, twin, and four-cylinder engine designs.

Test Cycle

For the verification of PEMS equipment, the utilization of an Real-Drive Cycle (RDC) is strongly recommended. This specialized driving cycles have been methodically designed to replicate real-world driving conditions within the controlled environment of a laboratory. The advantage of employing RDC for the verification process lies in its ability to represent a broader spectrum of operating conditions compared to cycles derived from regulatory standards, as demonstrated in Figure 4 for an exemplary L3e-A3 motorcycle. Unlike regulatory cycles that often represent limited power outputs and engine speed ranges, RDC significantly expands the operating range, providing a more accurate representation of real driving scenarios with flexible gear shifting.

The RDCs include a mix of different driving conditions such as acceleration, deceleration, cruising, and idling, thereby ensuring that the equipment is tested across a wide range of real-world situations, as shown in Figure 5 [11,13]. This makes it an ideal tool for validating the performance of the PEMS equipment [13], especially under dynamic load conditions that are not typically covered in regulatory cycles.

TABLE 2 list of investigated vehicles incl. main specs

vehicle [#]	cat. [-]	number of cylinders [-]	displacement per cylinder [ccm]	ign. spacing [°CA]	EU market share [%]
1	L3e-A1	1	125	720	0.355
2	L3e-A2	1	313	720	0.207
3	L3e-A2	1	373	720	0.224
4	L3e-A3	1	690	720	0.807
5	L3e-A2	2	199	360	0.087
6	L3e-A3	2	399	360	0.303
7	L3e-A3	2	445	360	1.005
8	L3e-A3	4	250	180	0.843

FIGURE 4 engine map highlighting the cycle dependent operational load points for an exemplary L3e-A3 motorcycles [13]

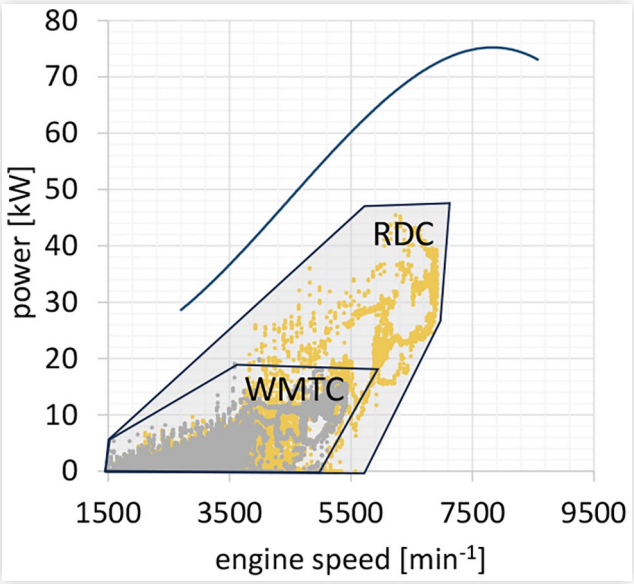

FIGURE 5 speed traces of different RDCs utilized for the correlation process

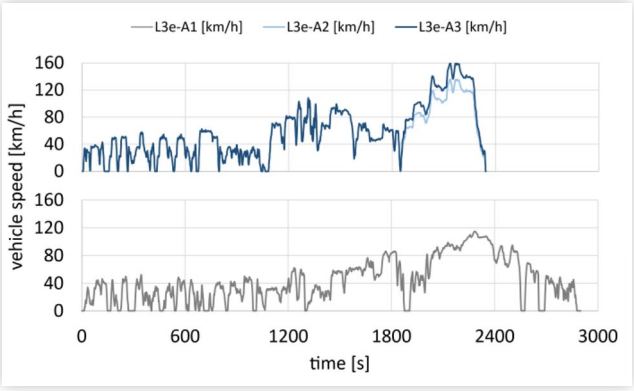

Data Analysis and Results

Correlation Analysis for Different Engine Configurations

This section assesses the correlation of the EFM measured flow to the reference (CVS) for different motorcycles, further engine architectures starting from small single cylinder engines all the way to high capacity four-cylinder engines. RDCs were used for all studies in this chapter, suited to the vehicles subclass.

Single-Cylinder Engines The regression analysis in Figure 6 shows the performance of the EFM (PEMS.exh. MF) compared to the reference measurement (CVS.exh.

FIGURE 6 correlation results of the EFM and the reference for single cylinder engine equipped motorcycles

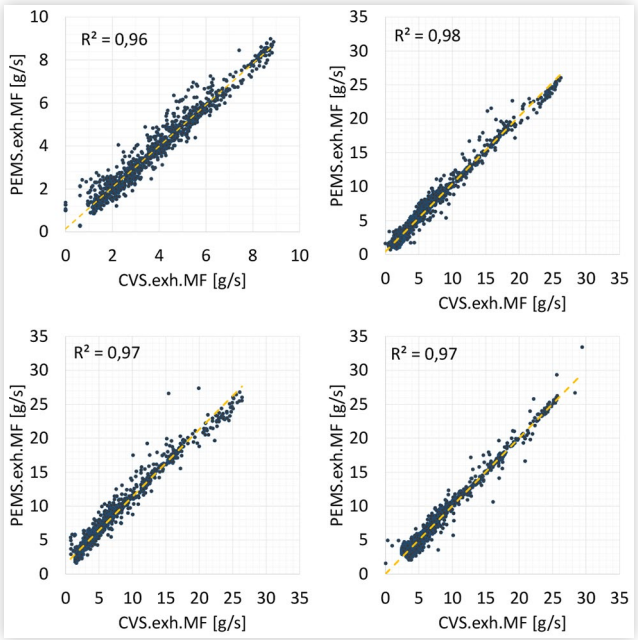

MF) for four single-cylinder engines with increasing displacement (125cc, 313cc, 373cc, 690cc). The analysis is based on the correlation coefficient R^2 and the dispersion of the measurement points relative to the ideal regression line. The results show a generally very good agreement between the two systems, with R^2 values of 0.96 to 0.98. Nevertheless, the measurement accuracy and scattering vary depending on the engine displacement and mass flow ranges.

The 125cc engine (Figure 6 top left, vehicle #1) has the lowest R^2 value (0.96) and the largest scattering of the measured values. There could be several reasons for this: First, smaller engines produce lower exhaust volume flows, which can affect the sensitivity of the EFM. Since measuring devices are more accurate for larger volume flows, fluctuations can occur more strongly at low flow rates, which is reflected in a "noise" in the measured values. Secondly, the exhaust gas flow is more pulsating in smaller single-cylinder engines, especially at low engine speeds. These pulsations are caused by the periodic exhaust gas output of a single cylinder and lead to varying pressure and flow values, which the EFM can only record with difficulty. In addition, relative measurement errors are more pronounced at very low flow rates, as small absolute deviations in this range have a greater relative effect. This combination of factors leads to lower precision and a wider spread of measured values.

The engines with larger displacements show better measurement results with R^2 values of 0.97 to 0.98. This is mainly due to the higher exhaust gas volumes and more uniform flow dynamics, which favor the stability of the measurement. In the medium mass flow range, which represents the typical operating state of the engines, the agreement between EFM and CVS is particularly high and scattering is minimal. However, these correlations also show pronounced scattering in the lower flow ranges.

In summary, the EFM shows good agreement with the reference in the medium measurement range, which indicates a high measurement accuracy in the usual operating conditions of the engines. The larger scatter at small displacements (125cc) and at low flow rates is due to physical effects such as pulsations, thermal fluctuations and relative measurement errors. Despite these limitations, the overall performance of the flowmeter remains very reliable, especially for applications in the medium operating range and engine capacities above 300cc.

Multi-Cylinder Engines The performance evaluation of an EFM compared to the reference was also conducted for two-cylinder engines with different displacements. The results, plotted in Figure 7 show even better agreement between the two systems, with correlation coefficients ranging from 0.97 to 0.98. This high level of correlation highlights the reliability of the PEMS system across various engine displacements and flow ranges.

Across all tested two-cylinder engines, the EFM demonstrates strong performance, particularly again in the medium to high exhaust flow ranges. In these regions, the data points are tightly clustered around the regression line, signifying minimal dispersion and high accuracy.

FIGURE 7 correlation results of the EFM and the reference for two- cylinder engine equipped motorcycles

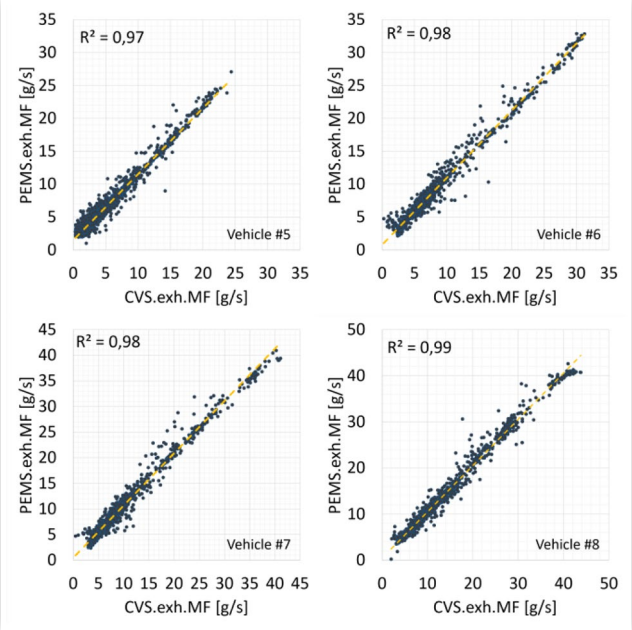

At lower flow rates, however, slightly more scatter is observed, although this effect is significantly less pronounced compared to single-cylinder engines. The smoother exhaust flow dynamics inherent to multi-cylinder engines contribute to this improvement in performance by reducing the influence of pulsations on the differential pressure-based measurement method of the EFM.

Pulsations in the exhaust gas flow arise from the periodic exhaust gas output of individual cylinders during the engine's combustion cycle. In single-cylinder engines, these pulsations are particularly pronounced due to the discrete, intermittent exhaust pulses and the absence of overlapping cycles. This creates fluctuating pressure and flow conditions that can challenge the sensitivity and stability of the EFM, especially at low flow rates. In contrast, two-cylinder engines inherently produce less pulsating exhaust flows because the firing cycles of the two cylinders overlap, resulting in a smoother and more continuous exhaust flow. This steadier flow improves the accuracy of the differential pressure-based measurement method, as the system is less affected by abrupt fluctuations in pressure and flow velocity.

The smallest two-cylinder engine (vehicle #5), with an R^2 value of 0.97, shows the greatest scattering among the two-cylinder engines, particularly at low flow rates. This is likely due to its relatively smaller exhaust gas volumes, which, while more stable than those of single-cylinder engines, are still subject to minor fluctuations that can affect measurement precision. Still, its performance is noticeably better than that of the 125cc single-cylinder engine (vehicle #1), demonstrating how the smoother flow dynamics of multi-cylinder configurations mitigate pulsation effects.

The 798cc engine (vehicle #6) achieves the best overall performance, with an R^2 value of 0.98 and minimal scattering across all flow ranges. This displacement aligns closely with the EFM optimal operating range, where exhaust flow volumes and dynamics enable high measurement precision. The 890cc engine (vehicle #7) also achieves an R^2 value of 0.98, though it shows slightly more scatter at higher flow rates. This increased scatter may result from the larger exhaust volumes, which amplify minor discrepancies in the measurement system.

In comparison to single-cylinder engines, two-cylinder engines exhibit consistently smoother exhaust flow dynamics, which enhance the performance of the differential pressure-based measurement method of the EFM. In single-cylinder engines, pulsations and their associated pressure fluctuations can significantly impact measurement accuracy, particularly at low flow rates. These pulsations not only introduce noise but also increase the likelihood of relative measurement errors, as small absolute deviations in low flow regions have a greater proportional effect. Conversely, the overlapping firing cycles of two-cylinder engines reduce the magnitude of these pulsations, creating steadier pressure conditions and enabling more accurate flow measurements, even at low flow rates. This distinction is particularly evident when comparing the performance of the EFM for the single-cylinder engine with that of the two-cylinder engine with almost same displacement (vehicle #2 and #5), where the latter exhibits significantly less scatter and greater overall accuracy.

The verification for a motorcycle with an in-line four-cylinder engine demonstrates the highest level of accuracy and reliability in exhaust flow measurement compared to single- and two-cylinder engine configurations. The in-line 4-cylinder engine (vehicle #8) achieved an R^2 value of 0.99, indicating an almost perfect correlation between the EFM and the reference. The regression line, with a gradient of 1, reflects a near-ideal alignment between the two measurement systems, and the scattering of data points around the regression line is minimal. This correlation is due to the superior flow dynamics of the four-cylinder configuration, which generates a continuous and smooth exhaust flow. The high frequency of exhaust gas pulses across four cylinders significantly reduces pulsations, enabling the differential pressure-based EFM to measure with exceptional precision across all flow ranges.

Investigations of Systematic Effects

The exhaust gas mass flow is directly proportional to the engine load and speed [15], making these parameters critical for evaluating the performance of exhaust flow measurement systems. To investigate potential systematic effects, the relative deviation between the EFM and the reference was analyzed across a broad range of operating conditions for one of the most challenging single cylinders equipped motorcycles.

To provide a comprehensive picture of the EFM behavior, averaged three-dimensional error surfaces were constructed based on engine load and speed (Figure 8a and 8b) for one exemplary vehicle (#2). This visualization highlights nonlinear interactions between mass flow determining operating parameters and measurement deviations. It reveals that the deviation is not a simple superposition of load- and speed-related components but includes distinct coupling regions where resonance effects, flow instabilities, and signal distortions coincide.

The three-dimensional error surfaces generated from the relative deviation between the EFM and the reference signal offer detailed insight into the combined influence of engine load and speed on measurement accuracy. Figure 8a shows the surface of the relative deviation across the load-speed map, highlighting characteristic regions of systematic error.

In the low-speed, low-load region of the operating map, large negative deviations are evident. These are attributed to very low absolute exhaust mass flows, which produce only minimal differential pressures across the sensor. As a result, the signal-to-noise ratio is unfavorable, and the EFM operates near the lower limit of its measurement range. Additionally, pulsating flow behavior becomes dominant under these conditions due to weak gas exchange and low mean flow momentum. In this regime, gas is primarily expelled by pressure gradients rather than actively displaced by the piston, which amplifies unsteady flow characteristics. Combined with the increased influence of noise and potential measurement lag, these effects lead to the observed systematic deviations.

To better understand the magnitude of the deviations, Figure 8b presents the absolute deviation over the

FIGURE 8a surface plot of the relative deviation between EFM and reference over engine load and speed for vehicle #2.

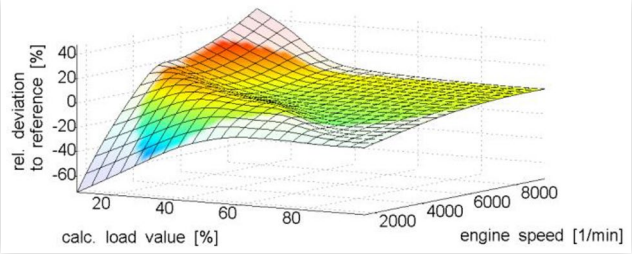

FIGURE 8b corresponding absolute deviation surface, highlighting areas of large error magnitudes for vehicle #2.

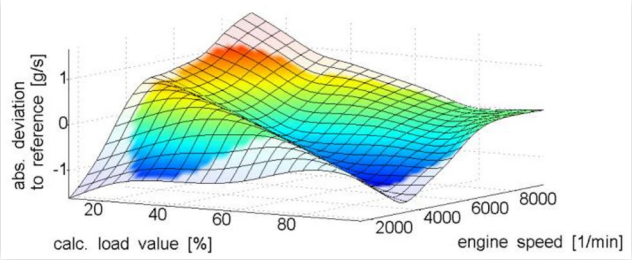

same operating range. It confirms that particularly large errors occur in the low-flow region, where sensor resolution and response time are most critical.

As load increases, the deviations tend to converge toward zero across a broad range of engine speeds. The exhaust mass flow rises, improving the signal-to-noise ratio and allowing the EFM to measure within its optimal dynamic range. The more continuous and higher-momentum flow reduces the impact of pulsations, while differential pressures become larger and more distinct from noise. This leads to more reliable measurements and improved agreement with the reference signal. Additionally, gas propagation times become shorter and more consistent, reducing the likelihood of phase-related errors.

A particularly striking feature of the error surface is a periodic, wave-like structure observed along the engine speed axis, which is not fully understood yet. This harmonic trend in the deviation is consistently present across multiple datasets and is independent of the reference source, confirming that it is intrinsic to the EFM system. The error fluctuates rhythmically with engine speed, with the magnitude of these oscillations decreasing at higher speeds. Since the exhaust pulse frequency - also known as the blow-down frequency - is directly proportional to engine speed, the EFM is subject to a frequency-dependent excitation pattern. This effect is further intensified by the non-sinusoidal shape of the exhaust mass flow, which introduces harmonics and sharp transitions into the signal. These high-frequency components can interact with internal sensor dynamics, digital filters, or resonant elements in the exhaust or probe geometry, potentially amplifying or attenuating specific frequency bands.

The ridge and valley structures in the error surface suggest the presence of resonance phenomena, where constructive or destructive interference occurs between the gas dynamic excitations and the measurement system response characteristics. Standing waves or resonant modes within the exhaust system—potentially caused by Helmholtz resonances, pipe reflections, or geometric features of the probe - could explain these features. Furthermore, as the speed of sound in exhaust gas depends on temperature, the timing of pressure and mass wave propagation varies with load and speed. These effects likely introduce non-linear, frequency-dependent phase shifts in the measurement chain.

Finally, the diagonal gradient visible in the 3D error plot indicates that the assumption of constant gas propagation delay may be oversimplified. The transit time of exhaust gas from the cylinder to the sensor is a function of instantaneous flow velocity, which itself depends on both engine speed and load. If this time delay is not correctly accounted for, systematic phase mismatches can occur, especially in transient or low-load regimes. Overall, the three-dimensional error surface reveals that the deviations are not merely the sum of independent load and speed effects, but rather the result of complex, coupled interactions involving gas dynamics, sensor response, and synchronization precision.

This hypothesis is further supported by a spectral analysis of the EFM signal from the RDC test. The EFM was positioned approximately 1.7 meters downstream of the exhaust valve. The resulting spectrogram (Figure 9) provides a time-frequency representation of the signal and reveals strong energy bands below 300 Hz.

These bands align with harmonics of the exhaust pulse frequency, which is determined by the blow-down events per second:

$$f_{fundamental} = \frac{n_{engine}}{60} \cdot \frac{z}{2} \tag{5}$$

where:

- z is the number of cylinders
- $\frac{1}{2}$ number of exhaust events per engine revolution

This results in a pulsation frequency that is directly proportional to engine speed, ranging from approximately 12.5 Hz at 1500 RPM to 58.33 Hz at 7000 RPM.

The presence of these harmonics in the spectrogram suggests that the sensor captures not only the fundamental exhaust pulse frequency but also its overtones, potentially due to non-sinusoidal waveform shapes (e.g., sharp pressure gradients or piston-induced flow asymmetry).

Moreover, nearly horizontal bands - i.e., frequency components that are independent of engine speed - suggest the presence of resonant modes within the exhaust system or sensor housing. These could be standing acoustic waves, Helmholtz-like resonances, or internal filtering effects in the sensor (e.g., due to the Annubar probe geometry or flow channels).

Such stationary resonances may interfere constructively or destructively with the speed-dependent excitation, depending on the operating point. This superposition of engine-induced and system-inherent frequencies could be a plausible explanation for the harmonic trend observed in the error plots across engine speed.

To address this phenomenon and improve accuracy without resorting to buffer volumes, several strategies can be employed. Signal filtering is one approach: low-pass

FIGURE 9 Spectrogram of measured exhaust mass flow over time for visualizing harmonic structures and stationary bands

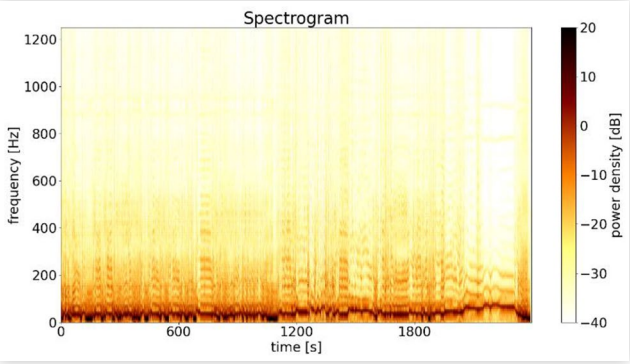

digital filters can effectively remove high-frequency pulsation noise above the dominant pulsation frequencies (e.g., 60 Hz), isolating the steady-state flow component. The filter frequency can be adapted in real time utilizing the engine speed information of the OBD port. Similarly, cycle-based ensemble averaging can reduce transient fluctuations by calculating the mean flow over multiple engine cycles. Adjustments to the sampling geometry, further the systems transfer function can also mitigate harmonic effects. Last, but not least a dynamic calibration of the system can improve the accuracy by assessing the setups transfer function in the calibration process.

Discussion

Interpretation of Results

The analysis of the Annubar-based 1.5" LF EFM for motorcycle exhaust flow measurement highlights both its strengths and its limitations. The investigation focused on its performance across a range of motorcycles, from 125cc single-cylinder engines to multi-cylinder powertrains, under various operating conditions.

One key finding is that, despite the challenging nature of pulsating exhaust flows, the EFM delivered promising results. Regression analysis between the EFM data and reference methods (either CVS or ECU calculated data) showed a strong correlation, with coefficients of determination (R^2) exceeding 0.96 in comparison with the CVS assessed mass flow. This indicates that, in general, the EFM provides reliable exhaust mass flow measurements across the operational range of all vehicles investigated. However, at very low flow rates, particularly during idle conditions, especially for small engine capacities, the EFM exhibited greater deviations from the reference. These discrepancies can be attributed to minimal deviation in differential pressure as well as the pulsating nature of exhaust flow at low speeds and loads, where low exhaust gas velocities and irregular flow patterns increase measurement uncertainty. The EFM principle of operation, which relies on differential pressure, struggles with the pronounced gas pulsations and low exhaust flow inertia in this regime.

Further analysis of systematic effects revealed a distinct pattern in the EFM relative deviation compared to reference measurements when plotted against engine parameters like load and speed (RPM). Oscillations in relative deviation were observed, particularly at low to mid engine speeds, even though the EFM has a high-frequency response of 5 kHz. The cause of these oscillations can be traced back to the interaction of exhaust gas pulsations with the sensor's response characteristics.

The results demonstrate that while the EFM can capture essential exhaust flow dynamics, systematic effects linked to engine pulsations present a unique challenge, particularly in single-cylinder engines. The EFM performs well for higher loads and speeds, where exhaust flow stabilizes and the effects of pulsations diminish. The oscillatory behavior at low speeds is an inherent aspect of single-cylinder engines and, to some extent, multi-cylinder engines with uneven firing intervals.

Potential Improvements

To address the identified limitations and enhance the performance of the Annubar-based EFM, some improvements can be proposed for future work.

One promising approach involves the application of advanced signal processing and filtering techniques. Although the EFM has a high frequency response of 5 kHz, the interaction with low-frequency engine pulsations is not adequately addressed in its raw form. The introduction of a Kalman filter or adaptive filters could offer significant benefits. These filters could be designed to recognize and compensate for harmonic disturbances caused by the exhaust pulsation frequency, especially in single-cylinder engines. Since the pulsation frequency is a direct function of engine speed and load, this information can be integrated into the filter design.

A specific approach could involve using engine speed (RPM) and load (both available from the OBD system) as inputs to the Kalman filter. The filter could use this information to predict the expected pulsation frequency and dynamically adjust the filter parameters to reduce its impact.

Additional improvement probably lies in the calibration process. Understanding the systems transfer function would be beneficial to better understand the effects of pulsation on the system and the response of the sensors. This information can be assessed by dynamic calibration.

Limitations of the Study

While the results are promising, the study does have clear limitations that must be acknowledged.

The EFM performance was verified using reference methods: the CVS method which was discussed in the methodology section but also ECU-calculated data. While these are well-established methods, they have their own limitations. CVS offers a lab-based reference, but does not offer high resolution, due to dilution effect and the inertia of the gas analyzers. Instead, ECU-calculated data are approximations of exhaust mass flow and are derived from sensor-based models rather than direct measurements, especially for motorcycles where MAF sensors are commonly not applied. The limited diversity of reference methods may influence the validation of EFM performance. Alternative reference methods, such as intake mass flow meters and/or fuel injection flow measurements, could provide higher resolution for better verification. However, such methods are often invasive, introducing backpressure or other disturbances that alter the engine behavior.

Summary/Conclusions

The present study demonstrated the feasibility of using an Annubar-based EFM for measuring exhaust mass flow in a range of motorcycle powertrains, including challenging single-cylinder low-capacity engines. The results showed high correlation with reference methods across various operating conditions. However, systematic deviations due to pulsations at low loads and speeds were observed, with oscillatory behavior in relative deviation most pronounced in the low-to-mid-speed range. These deviations are attributed to the interaction of engine pulsations with the EFM response characteristics.

To address these issues, future improvements could focus on signal filtering and engine-aware compensation techniques. Advanced filters incorporating engine speed and load data could dynamically adjusting, thereby, improving measurement accuracy.

The limitations of the study highlight the inherent challenges of non-invasive exhaust flow measurement, especially for low-speed single-cylinder engines. Nonetheless, the overall performance of the EFM was satisfactory for real-world application, and the results provide a foundation for further development. The ability to measure exhaust mass flow in real time has significant implications for real world emission testing.

By focusing on advanced filtering, dynamic compensation, and deeper exploitation of OBD data, future EFM designs could achieve better accuracy, especially in the lower-to-mid flow range where pulsations are most disruptive. These developments would make EFMs a viable method also for motorcycle RDE assessment.

References

1. Kulpe, M., Roß, T., Robel, C., and Atzler, F., "Exhaust Gas Mass Flow Determination on the Highly Dynamic Motorcycle Test Bench with PEMS," *MTZ Worldw* 82 (2021): 52-57. https://doi.org/10.1007/s38313-021-0666-7.
2. Mottram, R.C., "Introduction: An Overview of Pulsating Flow Measurement," *Flow Measurement and Instrumentation* 3 (1992): 114-117.
3. Matsuoka M., Hirai H., and Ito T., "Evaluation of Portable Emission Measurement Systems (PEMS) Accuracy by Simultaneous Measurement of PEMS and Laboratory-based Analyzers," *SAE International*, 2024.
4. Fonseca González, N., Casanova Kindelán, J., and López Martí, J.M., "NEZ, Methodology for Instantaneous Average Exhaust Gas Mass Flow Rate Measurement," *Flow Measurement and Instrumentation* 49 (2016): 52-62. https://doi.org/10.1016/j.flowmeasinst.2016.04.007.
5. Heywood, J.B., *Internal combustion engine fundamentals* (London [u.a.] McGraw-Hill: International ed., 1988).
6. Semlitsch, B., Wang, Y., and Mihăescu, M., "Flow Effects Due to Pulsation in an Internal Combustion Engine Exhaust Port," *Energy Conversion and Management* 86 (2014): 520-536. https://doi.org/10.1016/j.enconman.2014.06.034.
7. Annand W.J.D. and Roe G.E., "*Gas Flow in the Internal Combustion Engine: Power, Performance, Emission Control, and Silencing*," *GT Foulis*, 1974.
8. Hong, B., Venkataraman, V., Mihaescu, M., and Cronhjort, A., "Crank Angle-Resolved Mass Flow Characterization of Engine Exhaust Pulsations using a Pitot Tube and Thin-Wire Thermocouples," *Applied Thermal Engineering* 236 (2024): 121725. https://doi.org/10.1016/j.applthermaleng.2023.121725.
9. Silvis, W., Williamson, J., Kreft, N., and Alajbegovic, A., "DVE - Direct Vehicle Exhaust Flow Measurement using Head-Type Flowmeters," *SAE International* (2003).
10. Nakamura, H., Asano, I., Adachi, M., and Senda, J., "Analysis of Pulsating Flow Measurement of Engine Exhaust by a Pitot Tube Flowmeter," *International Journal of Engine Research* 6 (2005): 85-93. https://doi.org/10.1243/146808705X7329.
11. Hiesmayr J., Schmidt S., Hausberger S., Kirchberger R. et al., "Current Findings in Measurement Technology and Measurement Methodology for RDE and Fuel Consumption for Two-Wheeler-Applications."
12. Behrendt H., Mörsch O., Seiferth C.T., Seifert G.E. et al., "Studies on Enhanced CVS Technology to Achieve SULEV Certification," SAE Technical Paper Series, SAE International 400 Commonwealth Drive, Warrendale, PA, United States, 2002.
13. Schurl S., Keller S., Lankau M., Hafenmayer C. et al., "RDE Methodology Development for Motorcycle Emissions Assessment," SAE Technical Paper Series, Bangkok, Thailand, SAE International400 Commonwealth Drive, Warrendale, PA, United States, 2024.
14. "European Parliament and Council with Regard to Environmental and Propulsion Unit Performance Requirements and Amending," *Commission Delegated Regulation (EU) No 134/2014*, 2014.
15. Schurl S., Sturm S., Schmidt S., and Kirchberger R., "Novel Statistical Modelling-Based Approach for Exhaust Mass Flow Calculation in Motorcycles," SAE Technical Paper Series, Bangkok, Thailand, SAE International400 Commonwealth Drive, Warrendale, PA, United States, 2024.

Definitions/Abbreviations

ATDC - After Top Dead Center
CA - Crank Angle
CAN - Controller Area Network
CEL - Calculated Engine Load
CFO - Critical Flow Orifice
CVS - Constant Volume Sampler
ECU - Engine Control Unit
EFM - Exhaust Flow Meter
EPA - Environmental Protection Agency
EVC - Exhaust valve close

EVO - Exhaust valve open
DF - Dilution Factor
DR - Dilution Ratio
LF - Low Flow
MAF - Manifold Intake Air Flow
MAP - Manifold Intake Air Pressure
MAT - Manifold Intake Air Temperature
MF - Mass Flow
OBD - On-Board Diagnosis
PEMS - Portable Emission Measurement System
PFI - Port-Fuel Injection
RDC - Real Drive Cycle
RDE - Real Drive Emissions
RPM - Rotations Per Minute
STP - Standard Temperature and Pressure
WOT - Wide Open Throttle

Contact Information

Christian Hafenmayer
T +49 8374 2409 8514
M Christian.Hafenmayer@aip-automotive.de
W www.aip-automotive.de

AIP GmbH & Co. KG
Hoyen 30, 87490 Haldenwang, Germany

Stephan Schmidt
T +43 316 873 – 30153
M schmidt@ivt.tugraz.at

W www.ivt.tugraz.at

Graz University of Technology
Institute of Thd. and sustainable propulsion systems
Inffeldgasse 25b, 8010 Graz, Austria

ISSN 0148-7191